

CHEMISTRY OF MATERIALS

VOLUME 20, NUMBER 16

AUGUST 26, 2008

© Copyright 2008 by the American Chemical Society

Communications

Organic Field-Effect Transistors Based on Alkyl-Terminated Tetrathiapentalene (TTP) Derivatives

Yoshimasa Bando,^{*,†} Takashi Shirahata,[‡] Koji Shibata,[†] Hiroshi Wada,[‡] Takehiko Mori,^{*,‡} and Tatsuro Imakubo^{*,§}

Department of Organic and Polymeric Materials, Tokyo Institute of Technology, O-okayama, Meguro-ku, Tokyo 152-8552, Japan, Department of Chemistry and Materials Science, Tokyo Institute of Technology, O-okayama, Meguro-ku, Tokyo 152-8552, Japan, Imakubo Initiative Research Unit, Riken, Hirosawa, Wako, Saitama 351-0198, Japan

Received May 22, 2008

Revised Manuscript Received July 15, 2008

Organic field-effect transistors (OFET) have attracted much attention due to their potential application to flexible and inexpensive large-area electronics.¹ High-performance OFETs exceeding the mobility of $1.0 \text{ cm}^2 \text{ V}^{-1} \text{ s}^{-1}$ have been achieved in polyacenes and extended benzothiophene derivatives.² Tetrathiafulvalene (TTF) derivatives, which incorporate two sulfur atoms into the 1,3-dithiole ring in order to enhance the intermolecular interaction, are another family

of promising materials that have realized high performance.³ For further improvement of performance and stability, here we report a new skeleton of OFET materials, tetrathiapentalene (TTP),⁵ the compounds of which have considerably higher oxidation potentials than TTFs, that is expected to be advantageous to device stability. Although TTP compounds having more sulfur atoms in the outer rings have been extensively studied as components of organic superconductors,⁶ TTP compounds **1** and **2** capped with alkyl groups on both terminals have not been obtained via the ordinary routes.

[†] Department of Organic and Polymeric Materials, Tokyo Institute of Technology.

[‡] Department of Chemistry and Materials Science, Tokyo Institute of Technology.

[§] Riken.

(1) (a) Bao, Z.; Locklin, J., Ed. *Organic Field-Effect Transistors*; CRC Press: Boca Raton, FL, 2007. (b) Dimitrakopoulos, C. D.; Malenfant, P. R. L. *Adv. Mater.* **2002**, *14*, 99. (c) Facchetti, A. *Mater. Today*. **2007**, *10*, 28. (d) Murphy, A. R.; Fréchet, M. J. *Chem. Rev.* **2007**, *107*, 1066.

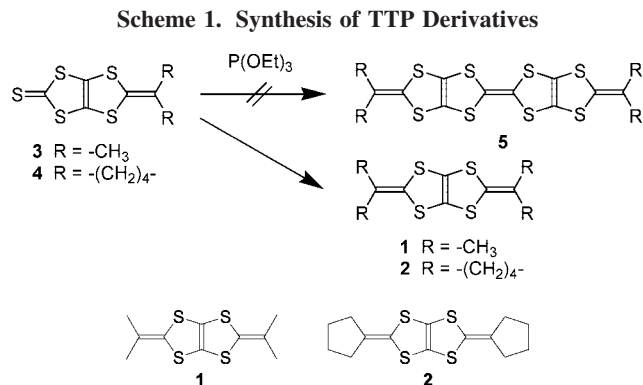
(2) (a) Klauk, H.; Halik, M.; Zschieschang, U.; Schmid, G.; Radlik, W.; Weber, W. *J. Appl. Phys.* **2002**, *92*, 5259. (b) Sundar, V. C.; Zaumseil, J.; Podzorov, V.; Menard, E.; Willett, R. L.; Someya, T.; Gershenson, M. E.; Rogers, J. A. *Science* **2004**, *303*, 1644. (c) Payne, M. M.; Parkin, S. R.; Anthony, J. E.; Kuo, C.-C.; Jackson, T. N. *J. Am. Chem. Soc.* **2005**, *127*, 4986. (d) Yamamoto, T.; Takimiya, K. *J. Am. Chem. Soc.* **2007**, *129*, 2224. (e) Ebata, H.; Izawa, T.; Miyazaki, E.; Takimiya, K.; Ikeda, M.; Kuwabara, H.; Yui, T. *J. Am. Chem. Soc.* **2007**, *129*, 15732.

(3) (a) Mas-Torrent, M.; Rovira, C. *J. Mater. Chem.* **2006**, *16*, 433. (b) Mas-Torrent, M.; Durkut, M.; Hadley, P.; Ribas, X.; Rovira, C. *J. Am. Chem. Soc.* **2004**, *126*, 984. (c) Mas-Torrent, M.; Hadley, P.; Bromley, S. T.; Crivillers, N.; Rovira, C. *Appl. Phys. Lett.* **2005**, *86*, 012110. (d) Naraso; Nishida, J.; Ando, S.; Yamaguchi, J.; Itaka, K.; Koinuma, H.; Tada, H.; Tokio, S.; Yamashita, Y. *J. Am. Chem. Soc.* **2005**, *127*, 10142. (e) Takahashi, Y.; Hasegawa, T.; Horiuchi, S.; Kumai, R.; Tokura, Y.; Saito, G. *Chem. Mater.* **2007**, *19*, 6382.

(4) Yamada, J.; Sugimoto, T. *TTF Chemistry*; Kodansha, Tokyo, 2004; pp 46–48.

(5) (a) Misaki, Y.; Nishikawa, H.; Kawakami, K.; Koyanagi, S.; Yamabe, T.; Shiro, M. *Chem. Lett.* **1992**, 2321. (b) Mori, T.; Kawamoto, T.; Misaki, Y.; Kawakami, K.; Fujiwara, H.; Yamabe, T. *Mol. Cryst. Liq. Cryst.* **1996**, *284*, 271.

(6) (a) Yamada, J.; Watanabe, M.; Akutsu, H.; Nakatsuji, S.; Nishikawa, H.; Ikemoto, I.; Kikushi, K. *J. Am. Chem. Soc.* **2001**, *123*, 4174. (b) Misaki, Y.; Higuchi, N.; Fujiwara, H.; Yamabe, T.; Mori, T.; Mori, H.; Tanaka, S. *Angew. Chem., Int. Ed.* **1995**, *34*, 1222. (c) Misaki, Y.; Nishikawa, H.; Kawakami, K.; Uehara, T.; Yamabe, T. *Tetrahedron Lett.* **1992**, *33*, 4321. (d) Misaki, Y.; Nishikawa, H.; Kawakami, K.; Koyanagi, S.; Yamabe, T.; Shiro, M. *Chem. Lett.* **1992**, 2321.



Compounds **1** and **2** were synthesized by phosphite-mediated coupling reactions of the starting materials, **3** and **4** (Scheme 1), which were prepared by the known Wittig reaction between a TTP-based phosphonate and the ketone.^{6c} The coupling reaction is likely to afford bis-TTP compounds **5**,⁷ but instead we obtained **1** and **2** with a single TTP unit in moderate yields (25–27%). The reaction mechanism is mysterious, but it is possible that a ring opening reaction of the 1,3-dithiol-2-thione part takes place after the attack by phosphite on the C=S bond (see the Supporting Information, Scheme S1). These compounds were purified by vacuum sublimation to give yellow-white powders. Thermal properties of **1** and **2** were investigated by differential scanning calorimetry (DSC) and thermogravimetric analysis (TGA), and no phase transition was found up to their respective decomposition temperatures at 210 and 223 °C.

The redox potentials were investigated by cyclic voltammetry (CV). The first redox potentials of **1** and **2**, +0.10 and +0.11 V (vs Fc/Fc⁺), respectively, are considerably higher than that of TTF (−0.08 V), meaning reduced donor ability.^{8a} This is a characteristic of the TTP skeleton.⁶ These values are, however, not much larger than those of double-TTF compounds with outer 1,3-dithiol rings,⁶ or that of BEDT-TTF (bis(ethylenedithio)tetrathiafulvalene) (+0.05 V).^{8b} The differences between the first and second oxidation potentials ($\Delta E = E_{\text{ox}}^2 - E_{\text{ox}}^1$) are 0.39 and 0.45 V for **1** and **2**, respectively, which are about the same as that of TTF (0.40 V). These observations indicate the inherent donor ability of the TTP skeleton, though it is slightly weaker than that of TTF. The obtained first redox potentials correspond to the HOMO levels, −4.90 and −4.91 eV below the vacuum level, which are slightly higher than that of pentacene (−4.85 eV).⁹ Optical HOMO–LUMO gaps are estimated to be 2.9 eV for both compounds from the absorption edges of the UV–vis spectra. This value is larger than that of dibenzo-TTF (2.40 eV),^{3d} and as large as those of the extended benzothiophene derivatives (2.9–3.0 eV),^{2d} which should be advantageous to stable transistor performance.

The transistors were fabricated by vacuum deposition on hexamethyldisilazane (HMDS)-treated Si/SiO₂ substrates, and showed typical p-type FET characteristics (Figure 1 and

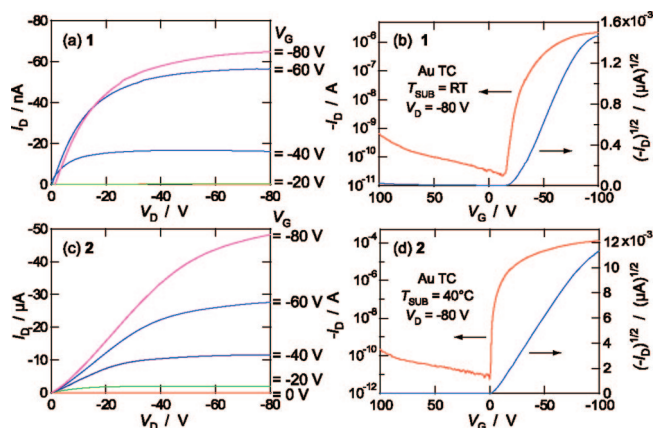


Figure 1. FET characteristics of (a, b) **1** and (c, d) **2** with TC Au electrodes on HMDS-treated Si/SiO₂ substrates deposited at rt and $T_{\text{sub}} = 40$ °C. Drain current I_D vs source-drain voltage V_D for (a) **1** and (c) **2**. I_D vs source-gate voltage V_G at $V_D = -80$ V for (b) **1** and (d) **2**.

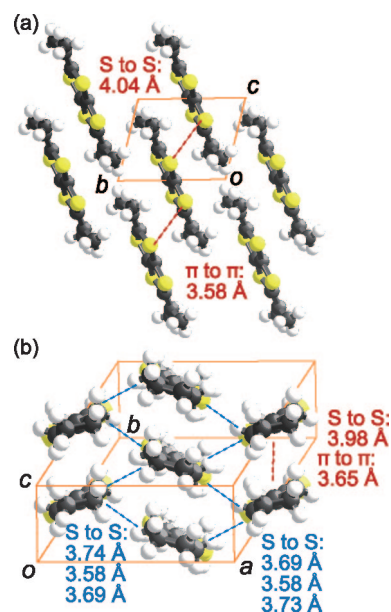


Figure 2. Molecular packings in the single crystals of (a) **1** and (b) **2**.

Table 1. FET Characteristics of **1** and **2**

S/D electrode		T_{sub}^a (°C)	μ^b (cm ² V ⁻¹ s ⁻¹)	$I_{\text{on}}/I_{\text{off}}$	V_{th}^b (V)
1	Au (TC)	rt	8.4×10^{-3}	$\sim 1 \times 10^5$	−27
	Au (BC)	rt	1.3×10^{-3}	$\sim 1 \times 10^4$	−35
	(TTF)(TCNQ) (BC)	rt	2.9×10^{-3}	$\sim 1 \times 10^4$	−33
2	Au (TC)	rt	0.12	$\sim 1 \times 10^6$	−1.6
		40	0.27	$\sim 1 \times 10^6$	−1.9
		60	4.1×10^{-2}	$\sim 1 \times 10^5$	−2.1
	Au (BC)	rt	5.8×10^{-3}	$\sim 1 \times 10^5$	1.3
		40	3.1×10^{-3}	$\sim 1 \times 10^4$	−2.7
	(TTF)(TCNQ) (BC)	rt	0.04	$\sim 1 \times 10^6$	−3.0
	40	0.17	$\sim 1 \times 10^6$	−1.6	

^a rt = room temperature. ^b Average data from more than five devices on the same substrate.

Table 1). Various devices were investigated by using Au and (TTF)(TCNQ) source and drain (S/D) electrodes with top-contact (TC) and bottom-contact (BC) configurations (Table 1), where TCNQ is 7,7,8,8-tetracyano-*p*-quinoxidimethane. (TTF)(TCNQ) electrodes give lower contact resistance and improve the performance of particularly BC transistors.¹⁰ The best performance was recorded for a device

(7) McCullough, R. D.; Petruska, M. A.; Belot, J. A. *Tetrahedron* **1999**, *55*, 9979.

(8) (a) Shizu, R.; Imakubo, T. *Chem. Commun.* **2003**, 3629. (b) Imakubo, T.; Shirahata, T.; Kibune, M. *Chem. Commun.* **2004**, 1590.

(9) Thelakkat, M.; Schmidt, H.-W. *Adv. Mater.* **1998**, *10*, 219–223.

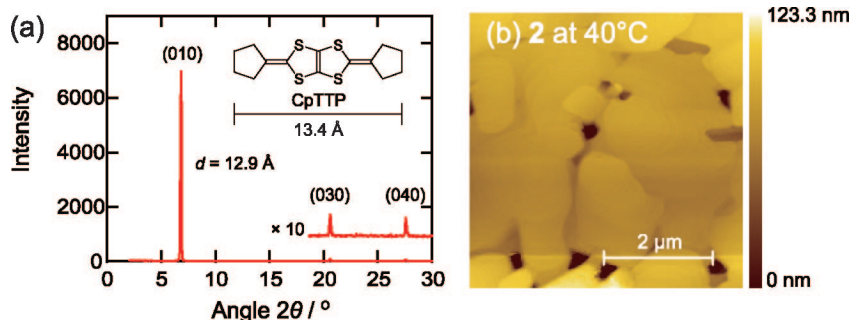


Figure 3. (a) XRD pattern and (b) AFM image of thin-film **2** deposited at 40 °C.

on which **2** had been deposited at $T_{\text{sub}} = 40$ °C, which showed a field-effect mobility μ of $0.27 \text{ cm}^2 \text{ V}^{-1} \text{ s}^{-1}$. It is noteworthy that the large on–off ratio of 10^6 and the small threshold voltage V_{th} come from the comparatively high oxidation potentials. Bottom-contact (TTF)(TCNQ) electrodes also attained nearly the same performance ($0.17 \text{ cm}^2 \text{ V}^{-1} \text{ s}^{-1}$). Compound **1** showed lower mobility by about two orders.

To investigate the molecular arrangements and the intermolecular interactions, we carried out single-crystal X-ray structure analyses of **1** and **2**.¹¹ The molecules of **1** are almost planar in the crystal, and construct uniform face-to-face π -stacking with interplanar π -to- π distance of 3.58 \AA along the c axis (Figure 2a). The molecules are, however, largely displaced along the molecular long axis, and considerably tilted from the stacking axis. There are several short S \cdots S distances in the side-by-side direction (3.71 \AA), whereas S \cdots S distance along the molecular stack direction is as large as 4.04 \AA (Figure 2a and the Supporting Information, Figure S3). The terminal cyclopentane rings of **2** are slightly twisted and the carbon atoms are deviated from the molecular plane by 0.55 \AA for C6, 0.24 \AA for C7, 0.29 \AA for C13, and 0.61 \AA for C14. The crystal of **2** has a herringbone structure with the π -to- π distance of 3.65 \AA and the dihedral angle of 128° (Figure 2(b)). This angle is closer to 155° in dibenzo-TTF than to 67° in sexithiophene.¹² The herringbone structure has several short S \cdots S distances (3.58 – 3.74 \AA) in the diagonal directions (Figure 2b), and realizes a two-dimensional molecular network. The tilted stacking structure of **1** and anisotropic S \cdots S contacts are associated with the relatively poor transistor performance.

The X-ray diffraction (XRD) diagrams of the thin films vacuum deposited on Si/SiO₂ substrates show a series of sharp peaks with d -spacings of 6.1 \AA for **1** and 12.9 \AA for **2** (Figure 3a). For **2**, the d -spacing corresponds to the b -axis of the single crystal. The molecules are standing nearly perpendicular to the substrate, in agreement with the 16° tilt angle estimated from the molecular length 13.4 \AA . For **1**, the observed d -spacing is much shorter than the molecular length (10.6 \AA), and the relation to the single-crystal lattice constants is not straightforward.

The atomic force microscopic (AFM) image exhibits large grains as shown in Figure 3b for **2**, and the grain size increases as the substrate temperature T_{sub} is elevated from room temperature to 40 °C. This is related to the good performance of the OFET (Table 1). The AFM image at $T_{\text{sub}} = 60$ °C, however, shows deep gap regions between the grains.

In summary, alkyl-capped TTP molecules were obtained by a phosphite-mediated contracting-coupling reaction, in which two TTP units merged into one. Compound **2** is a high-performance OFET material, the relatively high oxidation potential of which is responsible for both stability and small threshold voltage. It is notable that introduction of the outer ring system entirely changes the crystal and thin-film structures, and this is important in achieving the desired OFET properties.

Acknowledgment. The authors are grateful to Mr. M. Goto, Mr. Y. Watakabe, Prof. Ishikawa, and Prof. Takezoe for assisting with vapor deposition of Au, and to Mr. T. Sunohara, Mr. K. Yokomachi and Prof. Kakimoto for UV–vis, TGA, and DSC measurements. This work was partly supported by Grant-in Aid for Scientific Research (B) (18350095) and on Priority Areas of Molecular Conductors (15073211) from the Ministry of Education, Culture, Sports, Science, and Technology of Japan.

Supporting Information Available: Details for the synthesis and the physicochemical properties (TGA, DSC, UV–vis and CV) of **1** and **2**, the single-crystal structures of **1** and **2**, intermolecular interactions estimated from the extended Hückel molecular orbital calculations, the device fabrication, XRD diagrams and AFM images of the thin films (PDF); crystallographic information files (CIFs) for **1** and **2**. This material is available free of charge via the Internet at <http://pubs.acs.org>.

CM801404D

- (10) (a) Takahashi, Y.; Hasegawa, T.; Abe, Y.; Tokura, Y.; Saito, G. *Appl. Phys. Lett.* **2006**, *88*, 073504. (b) Shibata, K.; Wada, H.; Ishikawa, K.; Takezoe, H.; Mori, T. *Appl. Phys. Lett.* **2007**, *90*, 193509. (c) Shibata, K.; Ishikawa, K.; Takezoe, H.; Wada, H.; Mori, T. *Appl. Phys. Lett.* **2008**, *92*, 023305.
- (11) Crystallographic data of **1**: triclinic, $P\bar{1}$, $a = 6.419$ (2) \AA , $b = 8.081$ (3) \AA , $c = 6.116$ (2) \AA , $\alpha = 102.10$ (2)°, $\beta = 95.89$ (2)°, $\gamma = 106.87$ (3)° and $V = 292.3$ (1) \AA^3 . **2**: triclinic, $P\bar{1}$, $a = 10.608$ (7) \AA , $b = 13.666$ (6) \AA , $c = 5.216$ (2) \AA , $\alpha = 96.14$ (3)°, $\beta = 90.00$ (4)°, $\gamma = 72.13$ (4)° and $V = 715.2$ (6) \AA^3 in **2**.
- (12) Horowitz, G.; Bachet, B.; Yassar, A.; Lang, P.; Demanze, F.; Fave, J. L.; Garnier, F. *Chem. Mater.* **1995**, *7*, 1337.